Optical microscopic study of the stress induced corrosion of brass and aluminium in dilute electrolyte, and the inhibition effect of *Cedrus Atantica* and *Ocimum Basilicum*

Roland Tolulope Loto[1*], *Cleophas* Loto[1], and *Idorenyin* Usua [1]

[1]Department of Mechanical Engineering, Covenant University, Ogun State, Nigeria

Abstract. Optical microscopic analysis of the stress induced (85% calculated stress) corrosion of brass in 1M ammonium sulfate [$(NH_4)_2SO_4$] + 1M copper (II) sulfate ($CuSO_4$) solution, and aluminium in 0.5M, 1M and 2M sulfuric (H_2SO_4) solution at 10% and 20% addition of *Cedrus Atlantica* and *Ocimum basilicum Linn*. essential oil extracts were documented. The optical images obtained showed the effect of both extracts on the alloys. Optical images of aluminium in the presence of *Cedrus Atlantica* showed increased susceptibility of the alloy to localized and general corrosion compared to *Ocimum basilicum Linn* which enhanced the corrosion resistance of aluminium. *Cedrus Atlantica* increased the susceptibility of alpha brass to corrosion compared to the solution without it. In the absence of *Cedrus Atlantica*, general surface deterioration was observed without any localized corrosion. However, at 10% *Cedrus Atlantica* concentration superficial crack was observed. The crack further increased to visible intergranular crack (fracture) at 20% *Cedrus Atlantica* concentration. *Ocimum basilicum Linn* performed effectively at 10% concentration, sustaining the corrosion resistance of brass in 1M $(NH_4)_2SO_4$ + 1M $CuSO_4$ solution. At 20% *Ocimum basilicum Linn* concentration superficial cracking appeared.

1 Introduction

Corrosion has been a major industrial problem for centuries with increase in metallic alloy applications in various industries. The consequences of corrosion are adverse e.g. plant shutdown, contamination of the content of corroded packages etc. [1]. This phenomenon is the degradation or destruction by chemical or electrochemical means of metals and alloys in aqueous environment [2-5]. In corrosive environment, stress corrosion cracking mechanism crack development leading to unexpected sudden failure of normally ductile metals under tensile stress, especially at high temperatures [6]. This cracking mechanism is highly chemical-specific with respect to type of metallic alloys e.g. in chloride atmospheres stainless steels crack at relatively lower stress values [7]. Composition of the solution, type of metallic alloys, stress, and temperature are the major variables influencing stress corrosion cracking,

*Corresponding author: tolu.loto@gmail.com

hence metallic alloys demonstrating severe stress corrosion cracking, while filled with microscopic cracks, can appear bright and shiny [8]. This factor makes it common for stress corrosion cracking to propagate before failure undetected. Stresses can also be caused by crevice loads due to stress concentration or residual stress [9]. This shows stress corrosion cracking is a catastrophic form of environmental assisted corrosion, as the detection of fine cracks can be difficult at initial stage making it more difficult to predict [10]. Many alloys fail in chloride solutions, others in concentrated alkali and ammoniacal solutions. Environments in which cracking occurs have been found to be those in which corrosion is highly localized, usually without appreciable general surface corrosion. It has been shown that the composition of the corrosive environment has a basic and diverse influence on the stress corrosion cracking of the metallic alloys [11].

Corrosion inhibitors are substances added to corrosive environment in small quantities to prevent further degradation of metal [12]. Selection of corrosion inhibitors involves several factors such as cost, toxicity, availability, and environmental friendliness. Inhibitors are generally toxic, carcinogenic or even allergic, despite the high efficiency of many commonly used synthetic compounds. There has been an emerging need for biodegradable, environmentally friendly inhibitors with minimal health and safety concerns obtained from renewable resources [13]. Plant extract contains a wide range of organic compounds such as electron-rich atoms such as O, N, S, P, and multiple bonds or aromatic rings responsible for the formation of protective films formed on the metallic surfaces, thus preventing corrosion [14]. These extracts are environmentally safe compounds [8-10]. Research on biodegradable fluid derivatives and their potential use as corrosion inhibitors is growing [11–15]. This manuscript studies the effect of *Cedrus atantica* and *Ocimum basilicum linn* on the stress induced corrosion of α brass and aluminium in $(NH_4)_2SO_4$, $CuSO_4$ and H_2SO_4 solution.

2 Material and methods

2.1 Materials preparation

Aluminium (Al) and brass (Br) pipe samples were shaped into C-rings specimen. The outer diameter of Al is 40.25 mm with thickness of 0.195 mm and internal diameter of 37.1 mm. The outer diameter of Br is 50.3 mm with thickness 0.495 mm and internal diameter of 41.6 mm. The Al and Br specimens were manually cut to various parts from a long pipe and shaped into a c-ring with specific dimensions and measurements. The cut samples of Br and Al were drilled, a bolt was inserted into the drilled hole and the specimens were each stressed with the bolt and nut to tighten it to reduce the ring diameter of each specimen. The outside diameter of each specimen parallel to the stressed screw and wall thickness ware measured with a micrometer screw gauge. The C-ring test method was used for stress corrosion cracking of Al and Br. Each of the samples was taken out of the solution after every 48 h, washed with distilled water (H_2O) and acetone (C_3H_6O), then afterwards the specimens were left to dry and then weighed on the weighing balance. 0.5, 1M and 2M sulfuric acid (H_2SO_4) solution at 98% purity from sigma Aldrich was prepared from standard class H_2SO_4 acid solution in distilled H_2O. Mattson's solution was prepared from the admixture of 1M each of ammonium sulfate [$(NH_4)_2SO_4$] at 99% purity and copper(II) sulfate ($CuSO_4$) at 98% purity from Sigma Aldrich, at a ratio of 1:1. The Mattson's solution was made at a pH of 7.2. *Cedrus Atlantica* (CA) and *Ocimum basilicum Linn* (OBL) were added to 200 mL each of H_2SO_4 solution (0.5M, 1M and 2M H_2SO_4 solution) and Mattsson's solution as shown in Table 1.

Table 1. Solutions prepared for Al and Br alloys.

Designation of solution for Al		Designation of solution for Br	
A	0.5M H_2SO_4	A	1M $(NH_4)_2SO_4$ + 1M $CuSO_4$
B	1M H_2SO_4	B	1M $(NH_4)_2SO_4$ + 1M $CuSO_4$ + 10% CA
C	2M H_2SO_4	C	1M $(NH_4)_2SO_4$ + 1M $CuSO_4$ + 20% CA
D	0.5M H_2SO_4 + 10% CA	D	1M $(NH_4)_2SO_4$ + 1M CuSO4 + 10% OBL
E	1M H_2SO_4 + 10% CA	E	1M $(NH_4)_2SO_4$ + 1M CuSO4 + 20% OBL
F	2M H_2SO_4 + 10% CA		
G	0.5M H_2SO_4 + 10% OBL		
H	1M H_2SO_4 + 10% OBL		
I	2M H_2SO_4 + 10% OBL		

2.2 Calculations

Equation (1) was utilized to determine the stress applied to a C-ring specimen as given in Table 2:

$$OD_f = OD - \Delta,\ \Delta = \left(\frac{f\pi D^2}{4EtZ}\right) \quad (1)$$

where

- OD is the outer diameter of C-ring before any stress is applied, measured in in. (or mm).
- OD_f represents the outer diameter of the stressed C-ring, measured in inches (or mm), where *f* is the desired stress in MPa (or psi), provided it is within the proportional limit.
- Δ denotes the variation in outside diameter needed to achieve the expected stress, measured in mm (or in).
- D is the average diameter, calculated as (OD − t), in millimeters.
- *t* refers to the wall thickness, in millimeters (or inches).
- *E* represents the tensile modulus, measured in MPa (or psi).
- Z is the calibration factor applied for curved beams.

Table 2. Calculation of stress for Al and Br.

Al	Br
E = 10 x 106 psi (69 Gpa)	E = 14.79 x 106 psi (102 Gpa)
F = 4550.44 (85%). Stress was calculated at 85%	F = 10139.65 (85%). Stress was calculated at 85%
OD = 40.25 mm	OD = 50.3 mm
T = 0.195 mm	T = 0.495 mm
D = 40.055 mm	D = 49.805 mm
Z = 205.41	Z = $\left(\frac{D}{T}\right)$ 100.62

3 Results and discussion

3.1 Optical image analysis

Optical images of stressed Al alloys in 0.5 M H_2SO_4, 1 M H_2SO_4 and 2 M H_2SO_4 solution are shown from Figure 1(a) to 1(c). The images depict significant variation in morphology with respect to H_2SO_4 concentration due to the electrolytic action of SO_4^{2-} anion in the electrolyte upon dissociation of H_2SO_4 acid in H_2O. In Figure 1(a), the extent of deterioration is limited to relatively few corrosion pits. Increase in SO_4^{2-} anion concentration results in increase in the occurrence of corrosion pits as shown in Figure 1(b). The corrosion pits result from increased localized deterioration of Al surface especially at regions of flaws, impurities and inclusions. In Figure 1(c) the extent is surface deterioration has increased further with numerous corrosion pits and general corrosion deterioration. The general corrosion is due to the acidification of Al surface in the presence of the corrosive anions. Figure 2(a) to 2(c), and Figure 3(a) to (c) shows the stressed portion of Al in the presence of CA and OBL extract at 0.5 M, 1M and 2M H_2SO_4 solutions. The optical images in Figure 2 shows CA aggravates the conditions required for the deterioration of the Al alloy irrespective of H_2SO_4 concentration. Figure 2(a) to (c) shows the presence of extensive localized and pitting corrosion on the surface morphology of the alloy. This observation contrasts the observation in Figure 3 where Al images closely aligns with the images in Figure 1. However, the images in Figure 3 shows improved morphology and a more corrosion resistant surface compared to Figure 1.

Figure 4(a) and (b) shows the morphology of unstressed and stressed αBr from 1M $(NH_4)_2SO_4$ + 1M $CuSO_4$ solution. Significant variation in morphology is absent. However, in Figure 5(a) and (b) which shows the morphology of αBr from 1M $(NH_4)_2SO_4$ + 1M $CuSO_4$ at 10% and 20% CA, the presence of CA extract aggravates the conditions necessary for stress corrosion cracking to occur. At 10% CA, the crack is superficial occurring on the porous layer above the substrate alloy surface. The crack is the result of the combined action of corrodent and tensile stress [16]. Nevertheless, at 20% CA extract concentration, the crack has transited from superficial to deep-seated intergranular crack which occurred along the brain boundaries of αBr. The cracks probably started at corrosion sites on the material exterior and spreads into a brittle manner. Figure 6(a) and (b) shows the morphology of αBr in 1M $(NH_4)_2SO_4$ + 1M $CuSO_4$ at 10% and 20% OBL extract concentration. OBL extract significantly enhanced the stress corrosion resistance of αBr in 1M $(NH_4)_2SO_4$ + 1M $CuSO_4$ at 10% OBL concentration compared to 20 % OBL concentration. At 20% OBL concentration, superficial stress cracks appeared. The molecular configuration of *Ocimum basilicum linn* significantly differs from *Cedrus atlantica* with respect to interfacial interaction with Al alloy. The is the possibility of weak lateral attraction between the molecules of *Ocimum basilicum linn* and its inability to strongly adhere to the Al alloy surface in the presence of the corrosive species. This results in the corrosion of Al alloy as shown in the optical images. However, the observation contrasts the inhibition performance of *Cedrus atlantica* as shown in the images.

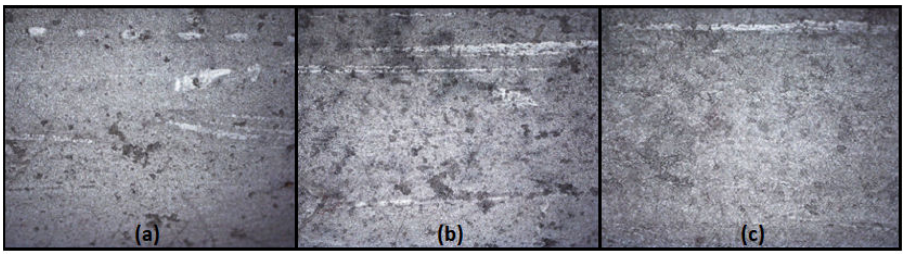

Fig. 1. Optical images of Al in (a) 0.5M of H_2SO_4, (b) 1M H_2SO_4 and (c) 2M H_2SO_4 after 192 h stressed.

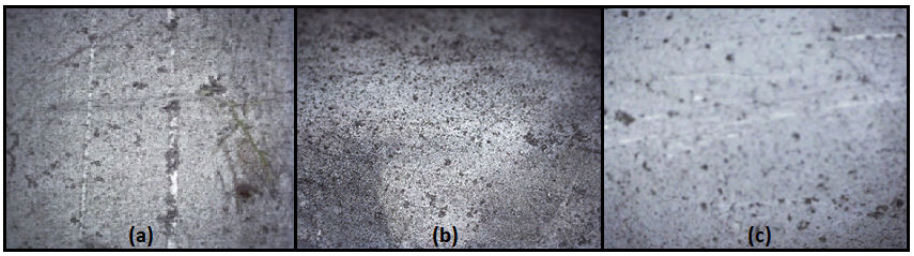

Fig. 2. Optical images of Al in (a) 0.5M of H_2SO_4, (b) 1M H_2SO_4 and (c) 2M H_2SO_4 after 192 h with stress of 85% in 10% CA.

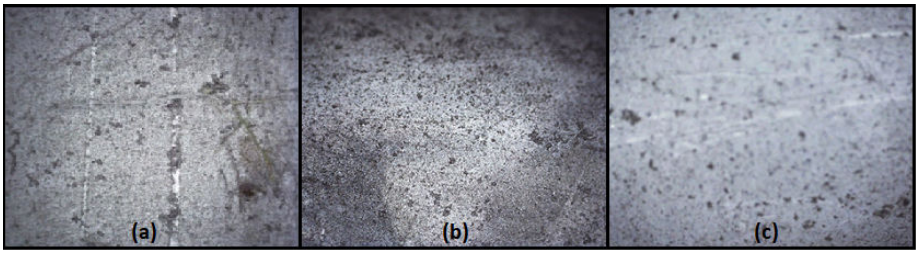

Fig. 3. Optical images of Al in (a) 0.5M of H_2SO_4, (b) 1M H_2SO_4 and (c) 2M H_2SO_4 after 192 h with stress of 85% in 10% OBL.

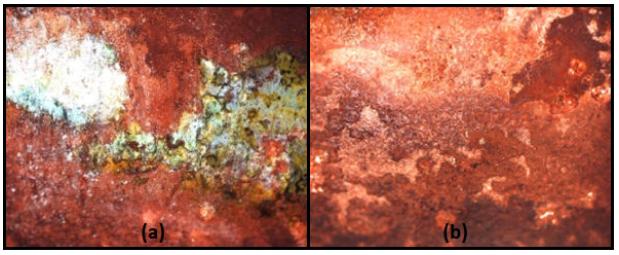

Fig. 4. Optical images of Br in 1M $(NH_4)_2SO_4$ + 1M $CuSO_4$'s solution after (a) 192 h unstressed, and (b) 192 h stressed by 85%.

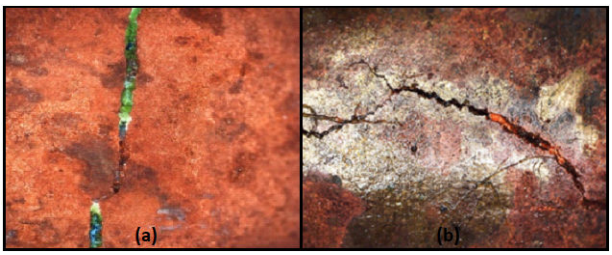

Fig. 5. Optical images of Br in 1M $(NH_4)_2SO_4$ + 1M $CuSO_4$'s solution after (a) 192 h stressed by 85% with 10% CA, and (b) 192 h stressed by 85% with 20% CA.

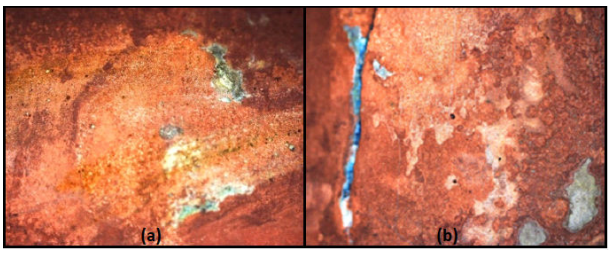

Fig. 6. Optical images of Br in 1M $(NH_4)_2SO_4$ + 1M $CuSO_4$'s solution after (a) 192 h stressed by 85% with 10% OBL, and (b) 192 h stressed by 85% with 20% OBL.

4 Conclusion

Cedrus Atlantica essential oil extract performed poorly on stressed aluminium and alpha brass metallic alloys in $(NH_4)_2SO_4$ + 1M $CuSO_4$ and H_2SO_4. The extract aggravated the conditions responsible for stress induced corrosion of the alloys. Corrosion pits were prevalent on aluminium and general surface deterioration was visible on alpha brass. *Ocimum basilicum Linn* enhanced the corrosion resistance of both alloys to stress induced corrosion. Surface deterioration present on the morphology of the alloys in the presence of *Cedrus Atlantica* were absent. However, at 20% concentration superficial cracks were observed.

The authors appreciate Covenant University for their financial support and provision of research facilities.

References

1. Z. Ahmad, Chapter 9 - Selection of materials for corrosive environment, principles of corrosion engineering and corrosion control, (Elsevier, Amsterdam, Netherland, pp. 479-549, 2006).
2. M.A. Fajobi, R.T. Loto, O.O. Oluwole, Corrosion in crude distillation overhead system: A review. J. Bio- Tribo-Corros. **5** (31), 67 (2019). https://doi.org/10.1007/s40735-019-0262-4
3. E.A. Keller, D.E. DeVecchio, Natural hazards: Earth's processes as hazards, disasters, and catastrophes, (5th Ed., Routledge, Oxfordshire, UK, 2019).
4. D. Landolt, Corrosion and surface chemistry of metals, (EPFL press, Lausanne, Switzerland, 2007).
5. P.R. Roberge, Corrosion Engineering. Principles and Practice, (1st Ed., Berkshire, United Kingdom, 2008).

6. F. Ellyin, Fatigue damage, crack growth and life prediction, (Springer Science & Business Media, Berlin/Heidelberg, Germany, 1997). https://doi.org/10.1007/978-94-009-1509-1
7. M.S. Darmawan, M.G. Stewart, Spatial time-dependent reliability analysis of corroding pretensioned prestressed concrete bridge girders, Struct. Saf. **29**(1), 16-31 (2007). https://doi.org/10.1016/j.strusafe.2005.11.002
8. M. Imran, Effect of corrosion on heat transfer through boiler tube and estimating overheating, Int. J. Adv. Mech. Eng. **4**(6), 629-638 (2014). https://www.ripublication.com/ijame-spl/ijamev4n6spl_06.pdf
9. S.J. Kline, N. Rosenberg, An overview of innovation. In studies on science and the innovation process: Selected Works of Nathan Rosenberg, World Scientific Pub Co Inc., Singapore, pp. 173-203 (2010). https://doi.org/10.1142/9789814273596_0009
10. J. Rajaguru, N. Arunachalam, Investigation on machining induced surface and subsurface modifications on the stress corrosion crack growth behaviour of super duplex stainless steel, Corros. Sci. **141**, 230–242 (2018). https://doi.org/10.1016/j.corsci.2018.07.012
11. J. Kovac, C. Alaux, T.J. Marrow, E. Govekar, A. Legat, Correlations of electrochemical noise, acoustic emission and complementary monitoring techniques during intergranular stress-corrosion cracking of austenitic stainless steel, Corros. Sci. **52**(6), 2015-2025 (2010). https://doi.org/10.1016/j.corsci.2010.02.035
12. C.A. Loto, R.T. Loto, Synergistic effect of tobacco and kola tree extracts on the corrosion inhibition of mild steel in acid chloride. Int. J. Elect. Sci. **6**(9), 3830 - 3843, (2011). https://doi.org/10.1016/S1452-3981(23)18292-7
13. R.T. Loto, T. Olukeye, E. Okorie, Synergistic combination effect of clove essential oil extract with basil and atlas cedar oil on the corrosion inhibition of low carbon steel, S. Afr. J. Chem. Eng. **30**, 28 – 41 (2019). https://doi.org/10.1016/j.sajce.2019.08.001
14. R.T. Loto, Anti-corrosion performance of the synergistic properties of benzenecarbonitrile and 5-bromovanillin on 1018 carbon steel in HCl environment. Sci. Rep. **7**(1), 17555, 2017. https://doi.org/10.1038/s41598-017-17867-0
15. M.G. Fontana. “Corrosion Engineering”, Tata McGraw-Hill Education India. 2005.
16. Y. Prawoto., A. Moin., M. Tadjuddin, W.B. Wan Nik, Effect of microstructures on SCC of steel: Field failure analysis case study and laboratory test result, Eng. Fail. Anal. **18**(7), 1858-1866 (2011). https://doi.org/10.1016/j.engfailanal.2011.06.015